Scaling Analysis of Nanowire Phase-Change Memory

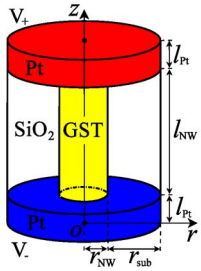
Jie Liu, Bin Yu, *Fellow, IEEE*, and M. P. Anantram

***Abstract*—This letter analyzes the scaling property of nanowire (NW) phase-change memory (PCM) using analytic and numerical methods. The scaling scenarios of the three widely used NW PCM operation schemes (i.e., constant electric field, voltage, and current) are studied and compared. It is shown that if the device size is downscaled by a factor of $1/k$ ($k > 1$), the operation energy (current) will be reduced by more than k^3 (k) times, and the operation speed will be increased by k^2 times. It is also shown that more than 90% of operation energy is wasted as thermal flux into substrate and electrodes. We predict that, if the wasted thermal flux is effectively reduced by heat confinement technologies, the energy consumed per RESET operation can be decreased from about 1 pJ to less than 100 fJ. It is shown that reducing NW aspect ratio helps decreasing PCM energy consumption. It is revealed that cross-cell thermal proximity disturbance is counter intuitively alleviated by scaling, leading to a desirable scaling scenario.**

***Index Terms*—Device scaling, electrothermal transport, nanowire (NW), phase-change memory (PCM), RESET current and energy.**

I. Introduction

THE NONVOLATILE phase-change memory (PCM) is promising to replace the Flash memory [1], [2]. As an alternative of the most popular thin-film PCM, novel nanowire (NW) and NW-like pore-shaped PCM research studies are gaining momentum in recent years [3]–[9]. However, in these emerging research studies, the NW radius, length, aspect ratio (AR), and operation scheme, which all exert significant impacts on device performance, are chosen largely at will and exhibit very large variance. To better understand and harness these influencing factors, and thereby to take advantage of the superior scalability of PCM technology, we present a unified scaling analysis of NW PCM performance by using both analytic and numerical methods. Our analysis reveals the promising scaling scenario by presenting the scaling laws of the crucial physical quantities, which determine the PCM device performance. This letter is inspired by the temperature scaling analysis in [10]. Our focus here is the diffusive transport region, in which the device dimension (tens of nanometers) is much larger than carrier mean free path $l_{\rm MFP}$ ($l_{\rm MFP} < 1$ nm [11]).



	c (J/m^{3}K)	κ (W/mK)	ρ (Ω·m)
GST	1.30×10^6	0.46	4.16×10^{-4}
SiO_2	1.94×10^6	1.40	1×10^{16}
Pt	2.84×10^6	71.6	1×10^{-7}

$R_{\rm th}$	20 m^{2}K/GW	**GST**	
$r_{\rm sub}$	400 nm	T_m	905 K
$l_{\rm Pt}$	200 nm	L	1.121 GJ/m^3

Fig. 1. (Left) Schematic of NW PCM geometry and (right) default parameters used in the simulation, i.e., specific heat capacity c, thermal conductivity κ, electrical resistivity ρ, $Ge_2Sb_2Te_5$ (GST) melting point T_m, GST latent heat L, and thermal boundary resistance $R_{\rm th}$ at GST–Pt interface and GST$-SiO_2$ interface.

II. Analytic Scaling Analysis

NW PCM research is still at its early stage, and the device operation schemes are diverse. To perform the RESET operations, the existing NW PCM work uses either constant current [4]–[6] or constant voltage [7]–[9] pulses. In addition, it was shown that the threshold switching of SET operations exhibits constant field scaling [6], [7]. Here, we will provide a general analysis and comparison of the scaling behaviors in the constant electric field, voltage, and current operation schemes.

In the cylindrical coordinate, as shown in Fig. 1, the governing equations of electrothermal transport in NW PCM before and after isotropic scaling are

$$\rho \boldsymbol{J}' = \boldsymbol{E}' = -\nabla' V' = -\nabla V \alpha = \boldsymbol{E}\alpha = \rho \boldsymbol{J}\alpha \tag{1}$$

$$c\partial_t T - \kappa r^{-1}\partial_r(r\partial_r T) - \kappa \partial_{zz} T - \rho J^2 = c\partial_{t'} T\beta - \kappa r'^{-1}\partial_{r'}(r'\partial_{r'} T)/k^2 - \kappa \partial_{z'z'} T/k^2 - \rho J'^2/\alpha^2 \tag{2}$$

where $r' = r/k$, $z' = z/k$ ($k > 1$), $t' = t\beta$. α is determined by how the electric field behaves with scaling in (1). β is chosen to keep (2) invariant after scaling. Here, we use the variables without (with) prime to denote quantities before (after) scaling. The meanings of the symbols are listed in Fig. 1 and Table I. We observe that i) if the electric field is kept constant in scaling ($\boldsymbol{E}' = \boldsymbol{E}$), (1) requires $\alpha = 1$ and $V' = V/k$; (2) is invariant if $T' = T/k^2$ and $\beta = 1/k^2$. As typical pulse duration is long enough for temperature to reach its steady state, making the pulsewidth longer than $t' = t/k^2$ will not increase the temperature beyond $T' = T/k^2$, and the PCM cell can never be switched to the RESET state. ii) If voltage is kept constant in scaling ($V' = V$), (1) requires $\alpha = k$; (2) is invariant if $T' = T$ and $\beta = 1/k^2$. This indicates that the

Manuscript received June 8, 2011; revised July 6, 2011; accepted July 11, 2011. Date of publication August 14, 2011; date of current version September 28, 2011. This work was supported by the U.S. National Science Foundation under Grant Award 1006182. The review of this letter was arranged by Editor T. Wang.

J. Liu and M. P. Anantram are with the Department of Electrical Engineering, University of Washington, Seattle, WA 98195 USA (e-mail: liujie@uw.edu; anant@uw.edu).

B. Yu is with the College of Nanoscale Science & Engineering, The State University of New York, Albany, NY 12203 USA (e-mail: byu@uamail.albany.edu).

Color versions of one or more of the figures in this letter are available online at http://ieeexplore.ieee.org.

Digital Object Identifier 10.1109/LED.2011.2162390

0741-3106/$26.00 © 2011 IEEE

TABLE I
ANALYTIC SCALING FACTORS

	Quantity	Const. E	Const. V	Const. I
r	radius	$1/k$	$1/k$	$1/k$
l	length	$1/k$	$1/k$	$1/k$
R	resistance	k	k	k
E	electric field	1	k	k^2
V	voltage	$1/k$	1	k
I	current	$1/k^2$	$1/k$	1
J	current density	1	k	k^2
T	temperature	$1/k^2$	1	k^2
t	time	$1/k^2$	$1/k^2$	$1/k^2$
P	power	$1/k^3$	$1/k$	k
Q	energy	$1/k^5$	$1/k^3$	$1/k$

temperature amplitude does not change, but the time required to reach the same amplitude is reduced by k^2 times [10]. iii) If current is kept constant in scaling ($I' = I$; hence, $\boldsymbol{J}' = \boldsymbol{J}k^2$), (1) requires $\alpha = k^2$ and $V' = Vk$; (2) is invariant if $T' = Tk^2$ and $\beta = 1/k^2$. This means that the temperature amplitude becomes k^2 times larger than that before scaling even if the pulse duration is reduced by k^2 times. Special attention should be paid to the sharply increased electric field $\mathbf{E}' = \boldsymbol{E}k^2$ because this intensifies electromigration, which limits the lifetime of a device.

The scaling factors are summarized in Table I. We can see that, in all of the three cases, t is scaled by a factor of $1/k^2$, indicating that the changing speed of T is k^2 times faster in the scaled PCM. Therefore, the RESET speed will be increased by k^2 times. The SET speed, however, is largely determined by crystallization speed, instead of the changing speed of T. Therefore, although experiment has shown that SET time can be reduced from about 100 ns to less than 10 ns if PCM cell size is scaled from 500 nm to less than 50 nm [3], a microscopic theoretical analysis is required to quantitatively define the impact of scaling on SET speed. Since RESET and SET operations adopt the constant voltage [7] and constant field [12] scaling, the RESET and SET energy Q (current I) scaling factors are $1/k^3$ $(1/k)$ and $1/k^5$ $(1/k^2)$, as shown in Table I.

III. NUMERICAL SCALING ANALYSIS

The aforementioned analytic scaling analysis reveals the benefits of scaling to reduce energy consumption and to increase device operation speed. However, first, it did not include the latent heat of melting; second, it scaled the thermal boundary resistance (TBR) $R_{\rm th} = -\Delta T/\kappa \nabla T$ artificially to $R'_{\rm th} = R_{\rm th}/k$. Here, ΔT means the temperature discontinuity ($\Delta T > 0$) at material interface. To overcome these drawbacks and obtain a more accurate scaling analysis, we numerically solve the Laplace equation $\nabla^2 V = 0$ to obtain the current density $\boldsymbol{J} = -\rho^{-1}\nabla V$. Then, the heat equation [see (2)] is solved for temperature distribution by using the time-dependent finite-element method (TD-FEM). In solving Laplace's equation, the Dirichlet boundary condition V_+ and V_- are applied at the top and bottom Pt surfaces, as shown in Fig. 1. In solving the heat equation, the Dirichlet boundary condition $T = 300$ K is imposed at the top and bottom Pt surfaces. At $r = 0$ and at $r = r_{\rm NW} + r_{\rm sub}$, the homogeneous Neumann boundary conditions are applied for both T and V. V_+ and V_- are chosen so that the maximum value of $T(r_{\rm NW}, z, {\rm t}_R)$ exceeds T_m because this ensures one cross section of NW is melted within pulse duration time t_R and then quenched to amorphous state at $t > t_R$ when the pulse is off.

By using the method outlined above and parameters shown in Fig. 1, the scaling behaviors of crucial physical quantities that determine NW PCM RESET performance are shown in Figs. 2 and 3. In these plots, $r'_{\rm NW} = 40/k$ nm; $l'_{\rm NW} = r'_{\rm NW} \times$ AR nm; and $\Delta t' = 20/k^2$ ns. The four components (radial heat loss into the SiO_2 substrate $Q_{\rm rad}$, axial heat loss into Pt electrodes $Q_{\rm axi}$, energy used due to heat capacity $Q_{\rm cap}$, and energy used due to latent heat $Q_{\rm lat}$) that determine RESET energy Q are plotted in Figs. 2 and 3(c). Here, $Q_{\rm rad}$ $(Q_{\rm axi})$ is obtained by integrating the thermal flux at the GST$-$$SiO_2$ (GST–Pt) interface. It is obvious that more than 90% of the RESET energy is wasted as thermal energy loss into substrate and electrodes. For example, for NW with $r_{\rm NW} = l_{\rm NW} = 20$ nm (leftmost points of Figs. 2 and 3 with AR = 1), $Q \approx 0.64$ pJ, which consists of $Q_{\rm rad} \approx 0.27$ pJ, $Q_{\rm axi} \approx 0.32$ pJ, $Q_{\rm cap} \approx 0.04$ pJ, and $Q_{\rm lat} \approx 0.01$ pJ. Only $Q_{\rm cap} + Q_{\rm lat} \approx 50$ fJ is necessary to achieve the RESET operations. The wasted $Q_{\rm rad}$ and $Q_{\rm axi}$ consume 92% of Q. Therefore, confining heat during a RESET operation has the potential to improve energy efficiency by one order of magnitude. To do this, one can either use substrate and electrodes with small effective κ or use materials that have a large TBR with chalcogenides [see insets in Figs. 2 and 3(c)]. Our simulation reveals that if the κ values of the Pt and SiO_2 regions are decreased by two orders of magnitude, the RESET energy (current) can be reduced by 60%–70% (40%–50%).

To more clearly reveal the quantitative scaling relations, the numerical scaling factors are listed in Table II. In Figs. 2 and 3(b) and Table II, we can see that RESET operation adopts constant voltage scaling roughly. The numerical scaling factors of E, V, I, J, P, and Q are slightly smaller than the corresponding analytic scaling factors shown in Table I. Therefore, Table I is a lower limit of the improvement in device performance during scaling. We have shown that in a constant voltage scheme, $T' = T$. This means that the thermal proximity effect is kept the same during scaling. However, this conclusion is based on $R'_{\rm th} = R_{\rm th}/k$. In the spatial scale of our interest (tens of nanometers), we expect $R'_{\rm th} \approx R_{\rm th} > R_{\rm th}/k$. Therefore, downscaling will alleviate the thermal proximity disturbance.

Figs. 2 and 3 and Table II tell us that the aforementioned scaling conclusions are valid for various AR values. Fig. 4 reveals that decreasing the AR reduces the energy required but at the cost of increasing I. As large I limits the cell selector size and, hence, the data density, we need to strike a balance between energy efficiency and data density to select an appropriate AR value.

In this letter, κ and $T_{\rm m}$ are chosen to be the bulk values. In the nanometer scale, κ (T_m) can be suppressed due to modified phonon dispersion (interfacial energy [4], [9]). Therefore, the scaling scenario will be even better than those listed in Table II and Figs. 2 and 3.

In our analysis, we have neglected barriers (Schottky or other barriers) at the Pt-NW interface, which can modify heat dissipation leading to hot spots. The temperature dependence of resistivity is also neglected. These issues deserve future investigation.

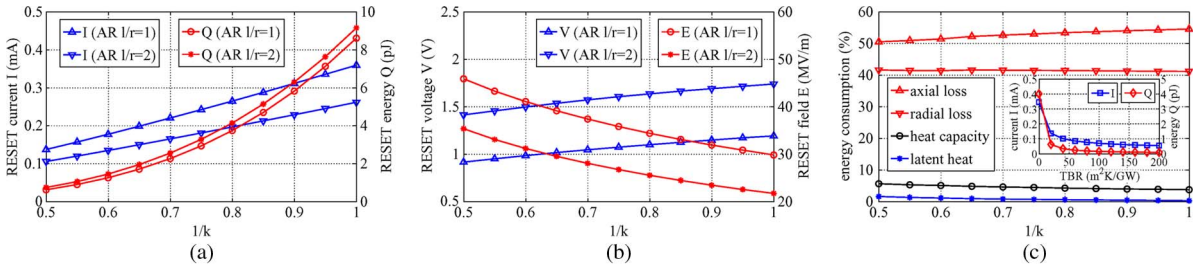


Fig. 2. RESET performance scaling of NW PCM with small AR ($l_{\rm NW}/r_{\rm NW}$) using TD-FEM. In (c), AR = 1.

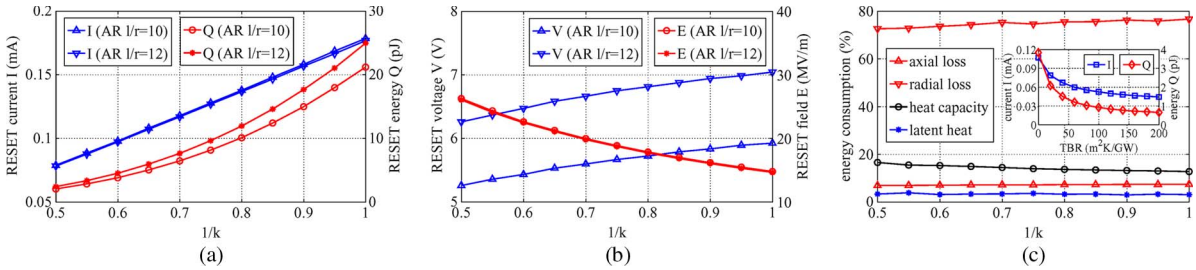


Fig. 3. RESET performance scaling of NW PCM with large AR ($l_{\rm NW}/r_{\rm NW}$) using TD-FEM. In (c), AR = 10.

TABLE II
NUMERICAL SCALING FACTORS ($k = 2$)

	Numerical Scaling Results						Analytic Scaling (Const. V in Tab. I)
	Small AR (Fig 2)		Medium AR		Large AR (Fig. 3)		
	AR 1	AR 2	AR 5	AR 6	AR 10	AR 12	
r	0.500	0.500	0.500	0.500	0.500	0.500	0.500
l	0.500	0.500	0.500	0.500	0.500	0.500	0.500
R	2.000	2.000	2.000	2.000	2.000	2.000	2.000
E	1.537	1.626	1.721	1.740	1.775	1.778	2.000
V	0.769	0.813	0.861	0.870	0.887	0.889	1.000
I	0.383	0.406	0.429	0.434	0.443	0.443	0.500
J	1.539	1.627	1.722	1.741	1.774	1.778	2.000
T	1.000	1.000	1.000	1.000	1.000	1.000	1.000
t	0.250	0.250	0.250	0.250	0.250	0.250	0.250
P	0.296	0.331	0.370	0.379	0.393	0.395	0.500
Q	0.074	0.083	0.093	0.095	0.098	0.099	0.125

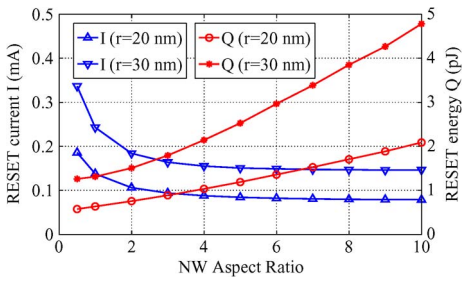


Fig. 4. Impact of AR ($l_{\rm NW}/r_{\rm NW}$) on RESET performance.

IV. CONCLUSION

A unified scaling analysis of the NW PCM under constant electric field, voltage, and current conditions has been presented. The impact of isotropic downscaling of device size by a factor of $1/k$ ($k > 1$) is investigated. We have shown that for the RESET operation i) constant electric field scaling is not a viable region of operation, ii) constant voltage scheme is desirable, iii) scaling alleviates cross-cell thermal proximity disturbance, iv) operation speed is increased by k^2 times, and v) operation energy (current) is reduced by more than k^3 (k) times. It has been demonstrated that more than 90% of the operation energy is wasted as thermal flux into substrate and electrodes. If heat can be effectively confined, the energy consumed per RESET operation can be reduced from about 1 pJ to less than 100 fJ.

REFERENCES

[1] P. H. Wong, S. Raoux, S. Kim, J. Liang, J. P. Reifenberg, B. Rajendran, M. Asheghi, and K. E. Goodson, "Phase change memory," *Proc. IEEE*, vol. 98, no. 12, pp. 2201–2227, Dec. 2010.

[2] G. W. Burr, M. J. Breitwisch, M. Franceschini, D. Garetto, K. Gopalakrishnan, B. Jackson, B. Kurdi, C. Lam, L. A. Lastras, A. Padilla, B. Rajendran, S. Raoux, and R. S. Shenoy, "Phase change memory technology," *J. Vac. Sci. Technol. B, Microelectron. Nanometer Struct.*, vol. 28, no. 2, pp. 223–262, Mar. 2010.

[3] W. J. Wang, L. P. Shi, R. Zhao, K. G. Lim, H. K. Lee, T. C. Chong, and Y. H. Wu, "Fast phase transitions induced by picosecond electrical pulses on phase change memory cells," *Appl. Phys. Lett.*, vol. 93, no. 4, pp. 043 121-1–043 121-3, Jul. 2010.

[4] B. Yu, X. H. Sun, S. Ju, D. B. Janes, and M. Meyyappan, "Chalcogenide-nanowire-based phase change memory," *IEEE Trans. Nanotechnol.*, vol. 7, no. 4, pp. 496–502, Jul. 2008.

[5] S. H. Lee, Y. Jung, and R. Agarwal, "Highly scalable non-volatile and ultra-low-power phase-change nanowire memory," *Nat. Nanotechnol.*, vol. 2, no. 10, pp. 626–630, Oct. 2007.

[6] M. Lankhorst, B. Ketelaars, and R. Wolters, "Low-cost and nanoscale non-volatile memory concept for future silicon chips," *Nat. Mater.*, vol. 4, no. 4, pp. 347–352, Apr. 2005.

[7] D. Yu, S. Brittman, and J. S. Lee, "Minimum voltage for threshold switching in nanoscale phase change memory," *Nano. Lett.*, vol. 8, no. 10, pp. 3429–3433, Oct. 2008.

[8] S. Meister, D. T. Schoen, M. A. Topinka, A. M. Minor, and Y. Cui, "Void formation induced electrical switching in phase-change nanowires," *Nano. Lett.*, vol. 8, no. 12, pp. 4562–4567, Dec. 2008.

[9] X. H. Sun, B. Yu, G. Ng, M. Meyyappan, S. Ju, and D. B. Janes, "Germanium antimonide phase change nanowires for memory applications," *IEEE Trans. Electron Devices*, vol. 55, no. 11, pp. 3131–3135, Nov. 2008.

[10] S. Kim and H. P. Wong, "Analysis of temperature in phase change memory scaling," *IEEE Electron Device Lett.*, vol. 28, no. 8, pp. 697–699, Aug. 2007.

[11] J. Lee, Z. Li, J. P. Reifenberg, S. Lee, R. Sinclair, M. Asheghi, and K. E. Goodson, "Thermal conductivity anisotropy and grain structure in $Ge_2Sb_2Te_5$ films," *J. Appl. Phys.*, vol. 109, no. 8, pp. 084 902-1–084 902-6, Apr. 2011.

[12] A. Pirovano, A. Lacaita, A. Benvenuti, F. Pellizzer, S. Hudgens, and R. Bez, "Scaling analysis of phase-change memory technology," in *IEDM Tech. Dig.*, 2003, pp. 29.6.1–29.6.4.